Size Dependence in the Stabilities and Electronic Properties of α-Graphyne and Its Boron Nitride Analogue

V. Ongun Özçelik*,†,‡ and S. Ciraci*,†,‡,§

†UNAM-National Nanotechnology Center, ‡Institute of Materials Science and Nanotechnology, and §Department of Physics, Bilkent University, 06800 Ankara, Turkey

ABSTRACT: We predict the stabilities of α-graphynes and their boron nitride analogues (α-BNyne), which are considered as competitors of graphene and two-dimensional hexagonal BN. On the basis of the first-principles plane wave method, we investigated the stability and structural transformations of these materials at different sizes using phonon dispersion calculations and ab initio finite temperature, molecular dynamics simulations. Depending on the number of additional atoms in the edges between the corner atoms of the hexagons, n, both α-graphyne(n) and α-BNyne(n) are stable for even n but unstable for odd n. α-Graphyne(3) undergoes a structural transformation, where the symmetry of hexagons is broken. We present the structure-optimized cohesive energies and electronic, magnetic, and mechanical properties of stable structures. Our calculations reveal the existence of Dirac cones in the electronic structures of α-graphynes of all sizes, where the Fermi velocities decrease with increasing n. The electronic and magnetic properties of these structures are modified by hydrogenation. A single hydrogen vacancy renders a magnetic moment of one Bohr magneton. We finally present the properties of the bilayer α-graphyne and α-BNyne structures. We expect that these layered materials can function as frameworks in various chemical and electronic applications.
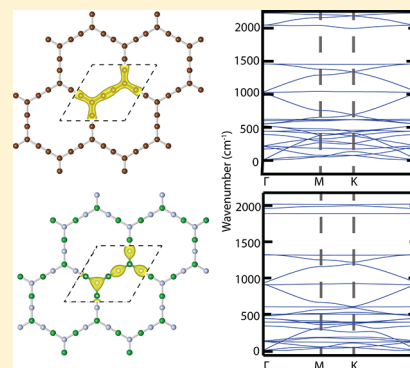
■ INTRODUCTION

The synthesis of graphene[1] has been an important turning point in the study of stable two-dimensional (2D) monolayer structures. Graphene has drawn great attention due to its properties such as high chemical stability, mechanical strength, and electric conductivity.[2,3] These unique electronic properties are mainly related to the Dirac cones present in its band structure where the upper and lower cones consisting of the conduction and the valence bands meet at a point on the Fermi level, making graphene a semimetal with zero band gap.

Graphynes, similar to graphene, are two-dimensional structures with the inclusion of single and triple bonded carbon atoms between the corner atoms of the honeycomb structure. Much earlier than the synthesis of single-layer graphene, Baughman et al.[4] predicted various flakes or molecules of carbon atoms in the graphyne family as layered phases using semiempirical and empirical atom—atom potential calculations. These finite size nanostructures form from the combination of hexagons with other polygons containing sp² and sp bonds. On the basis of first-principles plane wave calculation, Tongay et al.[5] have predicted various stable 1D, 2D, and 3D periodic structures containing carbon atomic chains. Among them, 2D periodic α-graphyne has been revealed. Very recently, band structures of the graphyne/graphdyne family with behaviors similar to that of single-layer graphene were calculated,[6] showing that neither the existence of hexagonal symmetry nor all atoms being chemically equivalent are prerequisites for the existence of Dirac point in the electronic structures.

Different types of the graphyne family are considered as a new class of 2D materials in the future era of carbon allotropes.[7] Finite-size building blocks of these graphyne structures have already been synthesized, which is an initial step toward extended structures.[8−13] Although extended (periodic) 2D structures of α-graphyne have not yet been synthesized, the synthesized finite-size flake building blocks are promising for future applications. Theoretical studies and simulations have revealed that different members of the graphyne family can lead to interesting electronic applications, and they can be used to construct graphyne-based frameworks and nanotubes. It is also possible to form the single layer, hexagonal boron nitride (h-BN)[14] analogues of certain types of graphyne, which are called BNyne throughout this manuscript.[6,15−18] Recently, effects of H, B, and N doping into graphyne structures were also investigated.[19] Additionally, the physical and chemical properties of graphyne and BNyne families and their future applications can be diversified by varying the sizes of rings and/or by functionalizing them with foreign ad-atoms.

Although graphyne allotropes have been widely studied in previous works, their stabilities have been an open question. In this paper, we investigate the stabilities of 2D periodic α-graphyne structures and their h-BN analogues by using first-principles calculations within density functional theory. An α-graphyne structure can be obtained by placing n number of
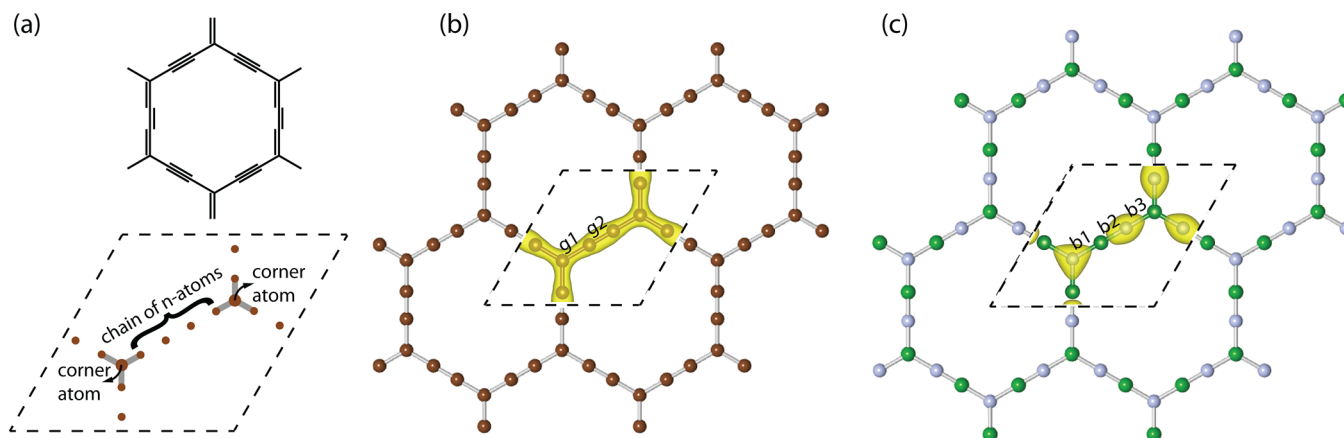
Figure 1. Atomic structure of α-graphyne and α-BNyne. (a) Schematic representation of α-graphyne(2) and the unit cell used to generate α-graphyne(n), where n is the number of carbon atoms placed between two carbon atoms located at the corners of the hexagon. Two corner atoms of the hexagon have a chain of n atoms between them, such that the unit cell contains 3n + 2 atoms. (b) Atomic structure of single-layer, 2D α-graphyne(2). The dashed lines delineate the primitive unit cell. The optimized bond lengths are g1 = 1.39 Å and g2 = 1.23 Å. The total charge density is shown within the unit cell. Carbon atoms are represented by brown balls. (c) Atomic structure of single-layer, 2D α-BNyne(2) with blue and green balls representing N and B atoms, respectively. The optimized bond lengths are b1 = 1.42 Å, b2 = 1.25 Å, and b3 = 1.44 Å. In the charge density plots, the isosurface value is taken as 0.2 electron/Å³.

carbon atoms between the corner atoms of the hexagonal graphene structure. We calculate phonon modes and perform ab initio, finite temperature molecular dynamics (MD) simulations to test the stabilities of different sized α-graphynes and α-BNynes. We investigate the electronic and mechanical properties of the stable structures. We find that the stabilities, the existence of Dirac points at the Fermi level, and the Fermi velocities of massless Fermions depend on the size of the α-graphyne, such that n = even cases lead to stable structures with graphene-like electronic structures, whereas n = odd cases lead to instabilities and eventually undergo structural transformations. In addition, the mechanical strengths of α-graphynes of various sizes (n = 2−4) were explored and compared with those of other honeycomb-like structures. We examine how the electronic properties are affected by hydrogen atoms adsorbed at the corner carbon atoms of hexagons, alternating from the top and bottom sides, and thus formed a structure analogous to graphane.[20] In addition, we provide a comprehensive comparison of cohesive energies with those of constituent 1D and 2D allotropes of carbon. We finally investigate the cohesive energies and electronic properties of bilayer structures of these materials. We also perform similar analysis for the h-BN analogues of graphynes, i.e., α-BNynes. Our study revealed a new, nonhexagonal α-graphyne structure, where the symmetries associated with hexagons are broken.

■ METHOD

In our calculations, we used the state-of-the-art first-principles plane-wave calculations within the density functional theory combined with ab initio, finite-temperature MD calculations using projector augmented wave potentials.[21] The numerical plane-wave calculations were performed using the VASP package.[22,23] The exchange correlation potential was approximated by the generalized gradient approximation with the van der Waals correction.[24,25] A plane-wave basis set with energy cutoff value of 600 eV was used. The Brillouin zone (BZ) was sampled in the k-space within the Monkhorst−Pack scheme,[26] and the convergence of the total energies and magnetic moments with respect to the number of k-points were tested. In the self-consistent total energy calculations and the MD

simulations, the BZ was sampled by $(17 \times 17 \times 1)$ mesh points in the k-space. The convergence criterion for energy was chosen as 10^{-5} eV between two consecutive steps. In the geometry relaxation and band structure calculations, the smearing value for all structures was taken as 0.01 eV. The pressure on each system was kept smaller than ∼2 kbar per unit cell in the calculations. In the ab initio MD calculations, the time step was taken as 2.5 fs, and atomic velocities were renormalized to the temperature set at T = 500 K and T = 1000 K at every 40 time steps. In the MD stability tests, the simulations were run for 5 ps. The phonon dispersion curves were calculated using plane-wave methods as implemented in the PWSCF package.[27]

■ α-GRAPHYNE AND α-BNYNE

Structure. We begin our analysis by investigating the structural and geometrical properties of α-graphynes at different (n) sizes. As shown in Figure 1(a), α-graphyne(n) structure has a hexagonal unit cell like graphene, but there are 3n + 2 carbon atoms in its unit cell instead of 2. In other words, we have the normal graphene-like structure with chains[28] consisting of n carbon atoms between the corner atoms of the hexagon on each side. Contrary to graphene, all of the C−C bonds are not equivalent to each other in these structures, but there exists bonds with different lengths and charge densities as shown in Figure 1(b). Variances of bonds originate from different types of bonding, sp² and sp¹ (+π), between carbon atoms. Therefore, the carbon atoms are no longer chemically equivalent to each other as they were in the case of graphene.

The h-BN analogue of this structure, namely, α-BNyne, can be easily obtained by replacing the carbon atoms with B and N consecutively. The electronegativity numbers of B and N atoms are 2.0 and 3.0, respectively, according to Pauling's electronegativity scale.[29] Hence, the electronic charge is transferred from B to the adjacent N in the ionic bonds of α-BNyne. Here, there are three different types of bonds: two at the corners of the hexagon and one at the center of edges. For B−N bonds at the corners, one is the case where N is at the corner of the hexagon and B in the edge as denoted by b1 in Figure 1(c), and the other is the opposite of this and denoted by b3. Note that, if

we want to preserve the 2D BN hexagonal structure such that the corner atoms of the hexagons are consecutively B and N, we must have an even number of atoms between the corner atoms. That is, we can only have n = even scenarios for the α-BNyne(n) cases. Odd n values would lead to either the same type of atoms on the corners of the hexagons or two identical atoms (B−B or N−N) next to each other. For this reason, we restrict ourselves with even n values for α-BNyne(n). The periodic geometries of these structures and the unit cells used to generate them are shown in Figure 1(b) and Figure 1(c) for α-graphyne(2) and α-BNyne(2) cases, respectively.

Stability. Up to now, finite building blocks of graphyne allotropes[8−13] and also the segments of atomic chains consisting of n carbon atoms[30−32] have been synthesized, which may be taken as an indication of the stabilities of their extended structures. Here, the main issue is whether the 2D single-layer, periodic structure of α-graphyne is stable or not. As an initial step we calculated the cohesive energies of these structures, which is defined as the energy required to form separated neutral atoms in their ground electronic state from the condensed state at 0 K and 1 atm.[33] Cohesive energies per atom of the carbon allotropes (namely, graphene, α-graphyne-(n), and cumulene or infinite carbon atomic chain[34]) are obtained using the expression

$$E_C = \{pE_T[C] - E_T[C_{allotrope}]\}/p \tag{1}$$

in terms of the optimized total energies of a single carbon atom in its magnetic ground state $E_T[C]$, and of the related carbon allotrope $E_T[C_{allotrope}]$, with p being the number of carbon atoms in the unit cell. In the case of BN structures, the cohesive energy is calculated per B−N pair using

$$E_C = \{qE_T[B] + qE_T[N] - E_T[BN_{allotrope}]\}/q \tag{2}$$

in terms of optimized total energies of a single B atom $E_T[B]$ abd N atom $E_T[N]$ and of the related BN allotrope, with q being the number of B−N pairs in the unit cell. Here (BN)$_{allotrope}$ stands for one of the structures, such as a BN chain,[35] h-BN, and α-BNynes. The calculated cohesive energies of graphene, α-graphyne(n), cumulene, and their h-BN analogues are given in Table 1. We note that the cohesive energies of α-graphyne(n) and α-BNyne(n) are smaller than their parent, single-layer graphene and h-BN honeycomb structures, respectively. Also expectantly, the cohesive energies of α-graphyne(n) and -BNyne(n) decrease with increasing n

Table 1. Cohesive Energies (E_C) of Optimized Graphene, α-Graphyne(n) (n = 1−4), Cumulene Structures, and Their h-BN Analogues[a]

structure	E_C (eV)
graphene	8.11
carbon chain	7.10
α-graphyne(1)	6.21
α-graphyne(2)	7.35
α-graphyne(3)	6.82
α-graphyne(4)	7.12
2D BN	14.52
BN chain	12.80
α-BNyne(2)	13.26
α-BNyne(4)	12.90

[a]The cohesive energies of the BN structures are given per number of B−N pairs.

since the cohesive energy of the linear atomic chain (either cumulene or BN) is smaller than the corresponding 2D single-layer, honeycomb structure (respectively, either graphene or h-BN). Like graphene and carbon atomic chains, the calculated cohesive energies suggest that α-graphyne structures correspond to local minima on the Born−Oppenheimer surface. Accordingly, even the network of carbon atomic chains consisting of a diverse number of atoms n, which are connected by three folded sp^2-orbitals at the nodes, can be in local minima.[36] In principle, these networks can form either multiply connected polygons(rings) or tree-like structure. Here we note that the cohesive energies of α-graphyne(n) for n = 1 and n = 3 calculated by restricting the structure in a plane are found smaller than that of n = 2 and n = 4. As clarified in the following analysis of stability using phonon calculations, n = odd number structures are unstable despite their positive cohesive energy. Here, smaller E_C for n = 1 and n = 3 relative to that of n = 2 and n = 4 indicates instability, but other analyses like calculation of phonon dispersion and MD simulations are needed for a reliable test of stability.

State-of the art calculations of phonon frequencies of α-graphynes and α-BNynes are carried out for all modes as a function of the k-points in the BZ. When the calculated frequencies of all the modes are positive, the structure is identified to be stable. We note that the constituent allotropes, namely, graphene, h-BN, carbon, and BN chains, have positive frequencies for all modes in their BZ, and hence they are stable. As seen in Figure 2, all calculated frequencies of α-graphyne(2)
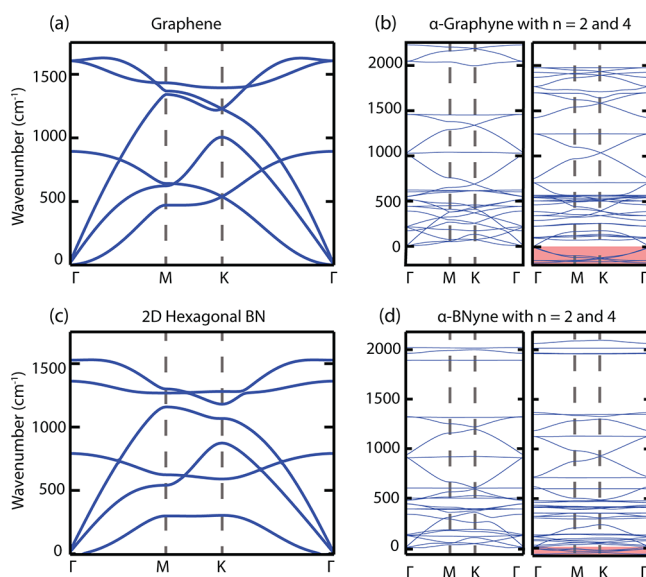

Figure 2. Calculated phonon bands. (a) Graphene. (b) α-Graphyne with n = 2 and n = 4. (c) Single-layer h-BN. (d) α-BNyne with n = 2 and n = 4. The dispersion curves for n = 2 have totally positive phonon modes which is an indication of their stability. On the other hand, n = 4 cases have modes with imaginary frequencies, which are marked with the shaded regions and will be discussed in the text. Phonon bands of unstable structures, such as n = 1 and n = 3, are not shown.

and α-BNyne(2) are positive. Moreover, due to the segments of atomic carbon and BN chains in α-graphyne(2) and α-BNyne(2), both structures have phonon modes with frequencies higher than those of single-layer graphene and h-BN. As a matter of fact, the maximum frequency of the
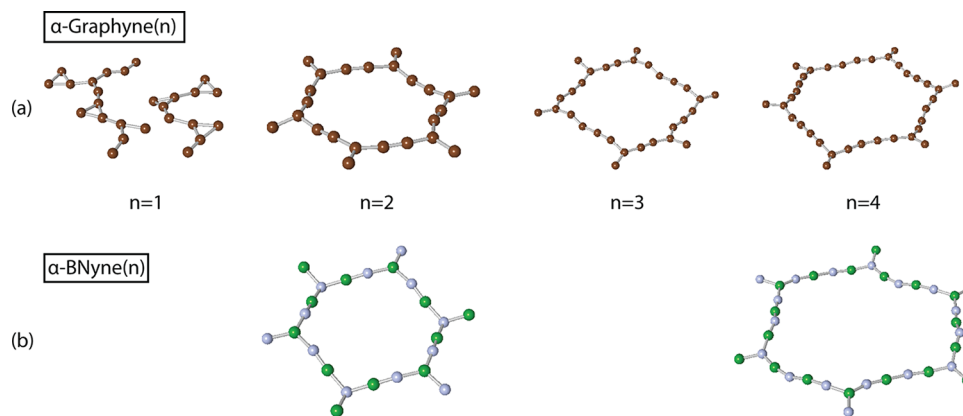
Figure 3. Snapshots of the MD simulations performed for 5 ps at $T = 1000$ K. (a) α-Graphyne(n) $n = 1-4$ structures. The structures are stable for $n = 2$ and $n = 4$, although buckled in the vertical plane. On the other hand, the $n = 1$ case breaks into carbon atomic strings and hence is totally unstable. α-Graphyne(3) undergoes a structural transformation, whereby it acquires stability by changing the number of C atoms to $n = 2$, $n = 3$, and $n = 4$ in the adjacent edges of hexagon. (b) Sections of α-BNyne(n). Both $n = 2$ and $n = 4$ cases remain stable during MD simulations. $n = 1$ and $n = 3$ cases are missed since α-BNyne(n) cannot be formed with odd n. Note that only a single ring from the periodic structures is shown here.

longitudinal optic mode (LO) of the carbon chain[36] can be as high as ~2400 cm^{-1}.

The situation is seemingly different for α-graphyne(4) and α-BNyne(4) since some of the acoustic modes have imaginary frequencies. These modes shaded out in Figure 2(b) and (d) correspond to imaginary frequencies and normally would indicate instabilities. However, the imaginary frequencies may arise also as an artifact of numerical calculations. To obtain the real frequencies of soft modes in an open structure comprising many atoms, one needs to perform calculations by taking into account the distant neighbors and use very high numerical accuracies. Thus, we believe that the calculated imaginary frequencies of soft modes in this case are artifacts of numerical phonon calculations since the segments of chains consisting of even carbon atoms have been found to be stable[36] and they become even more stabilized if they are connected to carbon atoms with three folded sp^2 orbitals. Also, it should be noted that all α-graphyne(n) and α-BNyne(n) with large n can be stabilized at finite size, since long-wavelength acoustical modes are discarded.

To further investigate the issue of stability, we performed MD simulations at $T = 1000$ K for 5 ps. The atomic structures obtained after the MD calculations are presented in Figure 3. It turns out that for $n = 2$ and $n = 4$ α-graphyne(n) and α-BNyne(n) remain stable after 5 ps of MD simulation even at high temperatures. Even though 5 ps is a short time interval, it is long enough for ab initio calculations at the temperature as high as $T = 1000$ K to provide evidence for stability. The analysis of atomic structures also suggests that α-graphyne(4) and α-BNyne(4) prefer to buckle in the vertical direction. Also in some cases, when specific structures are unstable in planar geometry they might undergo structural transformations to attain stability. Silicene (i.e., Si in graphene structure) is a crucial example for stability gained by buckling.[37] Here we ensure that the buckling occurs due to high temperature for the following reasons: (i) the optimization of buckled structure at $T = 0$ K ended with planar structure; (ii) similar buckling effects were also observed at segments of carbon atomic chains self-assembled on graphene and h-BN which bowed at high temperatures.[38−40]

It was found that α-graphyne(1) is totally unstable and is dissociated into carbon atomic strings. α-Graphyne(3) presents an interesting situation; it undergoes a structural transformation

and acquires stability by changing the number of carbon atoms to $n = 2$, $n = 3$, and $n = 4$ in the adjacent edges of hexagon as shown in Figure 4. This structural transformation is derived to
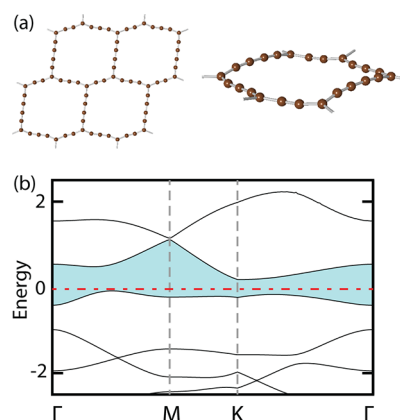

Figure 4. (a) Top and side views of the optimized geometry of the structurally transformed, stable α-graphyne(3). The planar, unstable α-graphyne(3) undergoes a structural transformation and acquires stability by breaking the symmetry of hexagons and eventually by buckling. The adjacent edges of the hexagon have $n = 2$, 3, and 4 carbon atoms, respectively. (b) Electronic structures of the buckled α-graphyne(3). The buckling leads to a gap opening of 0.42 eV.

maintain the proper bond order of finite size carbon chains constituting the edges of hexagon.[36] While the carbon atoms at the corners are always forming single bonds with the adjacent carbon atoms, the second atom from the corner by itself has to make a triple bond with the adjacent carbon atom, which is at the other side in the edge of the hexagon. At the end, the correct bond order of carbon atoms is preserved. However, this structural transformation, which modifies the geometric structure and breaks the symmetry of hexagons, reveals a new buckled allotrope carbon atom in 2D with a band gap of 0.42 eV.

Mechanical Properties. Having found the stable α-graphyne and α-BNyne structures, we next calculate their mechanical strengths. A common way of expressing the mechanical properties of two-dimensional materials is to calculate their in-plane stiffness, Poisson's ratio, and Young's
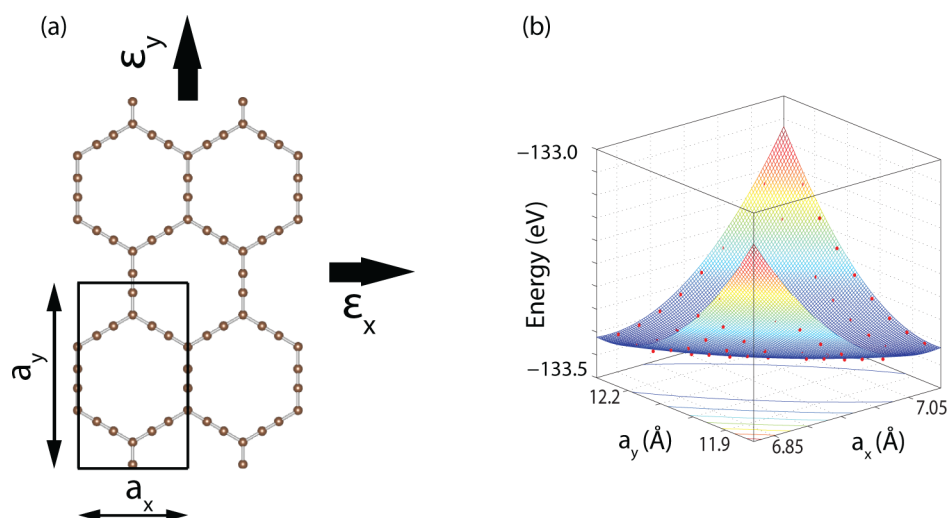
Figure 5. (a) α-Graphyne(2) structure in rectangular unit cell with its lattice constants a_x and a_y. ε_x and ε_y are the strains in x and y directions, respectively. (b) 3D plot of the energy values corresponding to different a_x and a_y values.
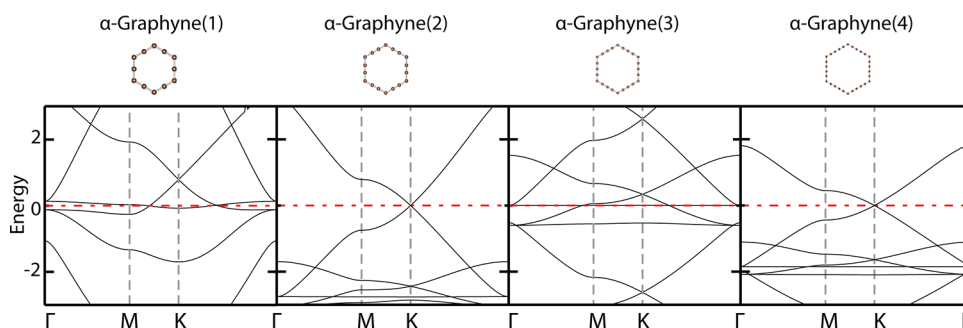

Figure 6. Electronic band structures of α-graphyne(n) for $n = 1, 2, 3,$ and 4. All of the band structures contain Dirac points, while they are shifted above the Fermi level for $n = 1$ and 3. $n = 1$ and 3 cases also have Dirac points away from the high symmetry K-point. The zero of energy is set to the Fermi level. Note that the electronic structures of the $n = 1$ and $n = 3$ structures are presented for the sake of completeness although they are unstable in the planar configuration, but the $n = 3$ structure acquires stability in the buckled geometry as discussed in the text.

modulus values. For this purpose, we used a rectangular unit cell in the xy-plane and applied tension in both x and y directions, as shown in Figure 5(a). We varied the lattice constants, a_x and a_y, between ±0.03% of the optimized values and calculated the energy value for each grid point obtained. In the end, we have obtained energy values for 225 grid points, which are plotted in Figure 5(b) for α-graphyne(2). The strain energy, E_s, at each point is calculated by subtracting the total energy at that point from the equilibrium total energy. It has been shown that this method of calculating the strain energy provides reliable predictions for graphene and 6−6−12 graphyne.[41−43]

The in-plane stiffness, which is a commonly used measure of strength for 2D materials, can be expressed as

$$C = \frac{1}{A_o} \times \frac{\partial^2 E_s}{\partial \varepsilon^2} \qquad (3)$$

where E_s is the strain energy; A_o is the equilibrium area; and ε is the axial strain calculated by $\Delta a_{x,y}/a_{x,y}$, a being the lattice constant in the x or y direction.

The in-plane stiffness values of α-graphyne(2), α-graphyne(4), α-BNyne(2), and α-BNyne(4) were calculated as 21, 16, 19, and 14 N/m, respectively. These values are much lower than the in-plane stiffness of graphene, which is ∼340 N/m.[41,44] As seen from these results, the implementation of new atoms

between atoms at the corners of hexagons decreases the mechanical strength of graphene dramatically, which is a direct consequence of the decrease in the average coordination number of carbon atoms. The Poisson ratio, which is defined as the ratio of the transverse strain to the axial strain, $\nu = -\varepsilon_{trans}/\varepsilon_{axial}$, was calculated as 0.88, 0.86, 0.89, and 0.85 for α-graphyne(2), α-graphyne(4), α-BNyne(2), and α-BNyne(4), respectively. By assuming an equivalent thickness with graphene, the Young's modulus values were calculated, respectively, as 61, 48, 52, and 42 GPa for these structures. We also note that in-plane stiffness, Poisson's ratio, and Young's modulus values of α-graphyne(n) and α-BNyne(n) decrease with increasing n. Also, the values calculated for α-BNyne(n) are lower than those calculated for α-graphyne for each case with equivalent n.

Electronic Structure. Earlier, Tongay et al.[5] showed that the electronic structure of α-graphyne(2) with two bands crossing the Fermi level at K- and K'-points of the BZ is similar to that of graphene. The presence of Dirac cones in the band structure of α-graphynes, as well as β-graphyne and 6−6−12 graphyne, have also been recently reported,[6] and it was demonstrated that the existence of Dirac points and cones is not a unique property of graphene. The crossing of bands at the Fermi level and the formation of Dirac cones were also investigated for other structures.[45] It was pointed out that bare structures, large defects, and ad-atoms on graphene can have

Dirac cones if their periodic patterns comply with a specific symmetry. Here, we present the electronic energy band structure of α-graphyne(n) for n = 1, 2, 3, and 4 in Figure 6. The existence of Dirac points is also seen here for all of these graphynes. Note that the Dirac point lies at the Fermi level for the stable n = 2 and n = 4 structures, whereas it is shifted above from the Fermi level for the unstable n = 1 and n = 3. We note that high electron density at the Fermi level of α-graphyne(n) for n = 1 and n = 3 can be attributed to their instability. The electronic energy near the K-point of the BZ is linear with respect to $\mathbf{q} = \mathbf{K} - \mathbf{k}$, which leads to

$$E(\pm) = \pm\hbar v_F \mathbf{q} + O[(\mathbf{q}/\mathbf{k})^2] \tag{4}$$

where v_F is the Fermi velocity and $\mathbf{K}$ is the wave vector corresponding to K- and K'-points of the BZ. Then, for the stable α-graphyne(2) and α-graphyne(4) structures, the first derivatives of their π bands near the K-point of the BZ were calculated as 29.4 and 23.4 eV Å, which have the same order of magnitude obtained for graphene, 34.6 eV Å . We also estimate the Fermi velocities as $v_F \sim 8.3 \times 10^5$ m/s for graphene, $v_F \sim 7.1 \times 10^5$ m/s for α-graphyne(2), and $v_F \sim 5.6 \times 10^5$ m/s for α-graphyne(4). Accordingly, the Fermi velocities at K- and K'-points decrease with increasing n. Noting the electron−hole symmetry of eq 4 near the K-point, α-graphyne(2) and α-graphyne(4) are found to be ambipolar. As discussed in the Stability section, α-graphyne(3) having a metallic state undergoes structural transformation where hexagons forming a honeycomb structure transform to rectangle-like structures as shown in the third panel of Figure 3. When planar, this structure attains high density of states at the Fermi level. However, through the buckling of the atomic structure, it undergoes a metal−insulator transition by opening an indirect band gap of 0.42 eV (see Figure 4).

On the other hand, reminiscent of the electronic structure of 2D single-layer h-BN, the band structures of α-BNyne(2) and α-BNyne(4) have wide band gaps as shown in Figure 7. It can be seen that the band gap decreases with increasing values of n. The lowest conduction band and the highest valence band states originate from B-p_z and N-p_z orbitals.
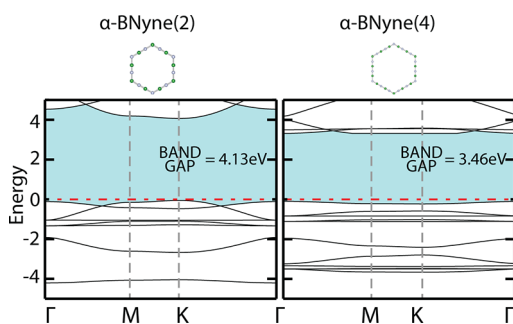

Figure 7. Electronic band structures of stable α-BNyne(n) for n = 2 and 4. Note that as n increases the band gap decreases. The maximum energy of the valence band is set to zero.

Hydrogenation. As an immediate application α-graphyne-(n) and α-BNyne(n), one may consider their chemical conversion through the coverage of H (hydrogenation), F (fluorination), and Cl (chlorination). Here we present our results regarding the hydrogenation of α-graphyne(2) and α-BNyne(2). The hydrogenation of graphene which produces graphane and the dehydrogenation of graphane are already

well-known processes.[20,46] Subsequently, hydrogenation of single-layer BN was also theoretically studied which leads into BN-phane.[47] In a similar way, we attach single hydrogen atoms to the corner carbon atoms of α-graphyne(2) and B and N atoms at the alternating corners of α-BNyne(2) from top and bottom alternately, as illustrated in Figure 8(a,b). Upon
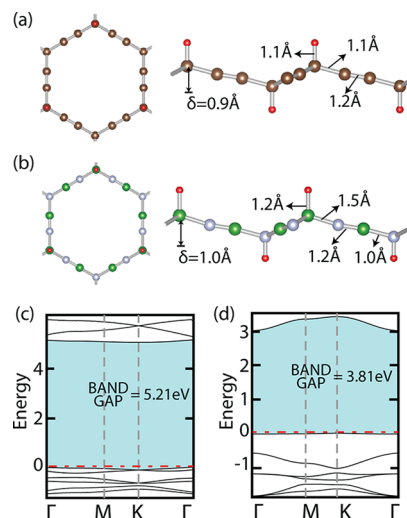

Figure 8. (a,b) Hydrogenated α-graphyne(2) and α-BNyne(2). Top and side views of the optimized hydrogenated structures are shown by the ball and stick models, where C, N, B, and H atoms are represented by brown, blue, green, and red balls, respectively. (c,d) Electronic structures of hydrogenated α-graphyne(2) and α-BNyne(2). Note that, in contrast to the semimetallic α-graphyne(2), the hydrogenated structure has a wide band gap of 5.2 eV. The maximum energy of the valence band is set to zero.

hydrogenation, both α-graphyne(2) and α-BNyne(2) structures relax into a buckled geometry with buckling distances of 0.92 and 1.03 Å. These buckled geometries are similar to the buckled geometries of graphane and BN-phane. However, the buckling increases from 0.45 to 0.92 Å as we go from graphane to hydrogenated α-graphyne(2), as a result of the increased length of the edges of hexagons. Hydrogenation also alters the electronic structures of these systems, as presented in Figure 8(c,d). Consequently, the semimetallic α-graphyne(2) structure attains a wide band gap of 5.2 eV upon hydrogenation. While hydrogenated α-graphyne(2) has a nonmagnetic ground state, a single hydrogen vacancy renders a magnetic moment of 1 μ_B

Hydrogenated α-BNyne(2) also has a wide band gap of 3.3 eV. The band gap opening effect of hydrogenation on monolayer structures is in accordance with prior calculations on graphane[46] and hydrogenated BN,[47] which have band gaps of 3.5 and 4.8 eV, respectively.

Bilayer Structures. Here we address the question of whether α-graphyne and α-BNyne can form layered structures similar to graphite and hexagonal BN, or not. We place their bilayers as shown in Figure 9 and explore equilibrium geometries, binding energies, and electronic structures. We begin the analysis by placing two single layers of α-graphyne(2) sheets on top of each other with AA stacking (i.e., hexagons in both layers face each other) and AB stacking (i.e., first layer is shifted laterally to the centers of hexagons in the second layer) geometries. We alter the interlayer distances until we achieve the minimum energy values. The calculated minimum energy geometries indicate that AB type of stacking is more favorable
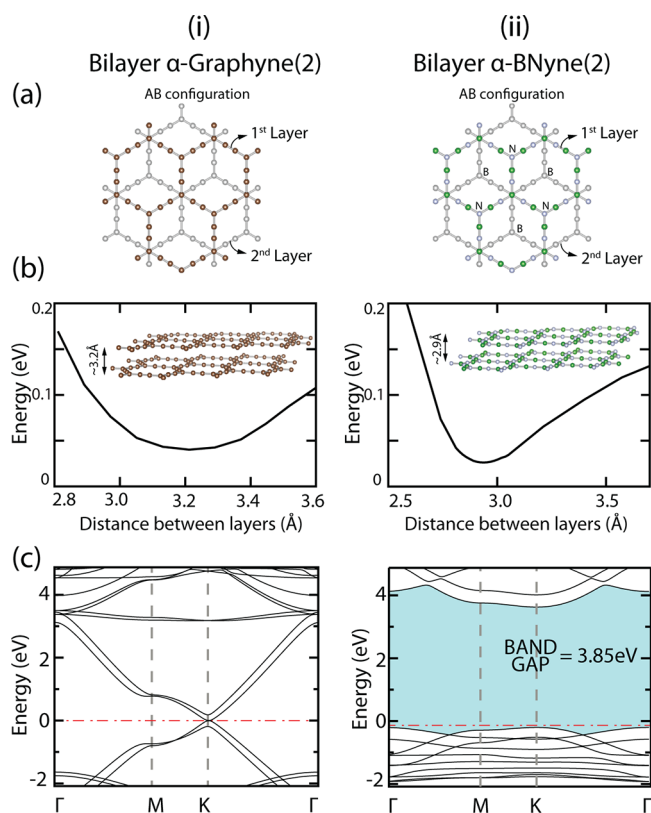
Figure 9. Bilayer α-graphyne(2) and its BN analogue bilayer α-BNyne(2) are shown in columns (i) and (ii), respectively. (a) Top view of the optimized two-layer structures. Both bilayer α-graphyne and α-BNyne have AB type of stacking geometry, which is more favorable than the AA stacking. In the ball and stick model C, B, and N atoms, respectively, are represented by brown, green, and blue balls, and all of the atoms in the bottom layer are shown in gray balls. (b) Variation of energy as a function of the layer−layer distance. (c) Electronic band structures of α-graphyne(2) and α-BNyne(2).

than AA type by 46 meV. This is a behavior similar to bilayer graphene structure or graphite. The optimized interlayer distance is calculated as 3.12 Å, which is less than the interlayer distance of graphite, 3.35 Å. This is mainly related to the less dense arrangement of carbon atoms on the graphyne surface as compared to the graphene, which results in lower surface energy and hence closer equilibrium distance. Similar results were also found in a previous interlayer distance and stacking studies made on different graphyne allotropes.[42,48]

A convenient procedure for calculating the interlayer binding energy for layered structures is subtracting the minimum energy of the bilayer structure from the sum of energies of separated individual layers.[49] Applying this method, we calculate the binding energy of bilayer α-graphyne(2) as 220 meV (27.5 meV/atom). We repeat the same analysis for bilayer α-BNyne(2), which also has an AB type double layer geometry as shown in the second column of Figure 9(a). For this case, the energy difference between AB stacking and the AA stacking is in favor of AB by 70 meV; the interlayer distance is 2.9 Å; and the binding energy is 128 meV(16 meV/atom). The calculated binding energies of bilayer α-graphyne(2) and bilayer α-BNyne(2) are in the range of the calculated binding energies of bilayer graphene (48 meV/atom) and bilayer h-BN (31.5 meV/atom), respectively. The variations of total energies around the minimum energy values as a function of the interlayer distances are shown in Figure 9(b). Like graphite and layered BN, small

interlayer binding energies consist of mainly from the van der Waals interaction with an even smaller chemical interaction component. Nevertheless, such a weak binding is enough to maintain the bilayer structure at low temperature. Additionally, 3D layered structures of α-graphyne and α-BNyne can form at room temperature. These arguments are corroborated by the MD simulations performed at different temperatures showing that the bilayer structures form stable interlayer binding near room temperature, but the layers move away from each other at high temperatures (T = 500 and 1000 K). These results imply that multilayers of α-graphyne and α-BNyne, even their 3D layered structures, can form.

We finally calculate the electronic structures of these double-layered structures. The band structure of bilayer α-graphyne(2) is shown in Figure 9(c). Note that the bands are split due to the couplings between layers, and the numbers of energy bands are doubled as compared to the single α-graphyne(2) sheet. Notably, the bands are no longer linear around the K-point, but parabolic. This kind of structure is reminiscent of the electronic structure of bilayer graphene or graphite.[50] As opposed to a single layer, the bands no longer touch at the K-point, but there is a small band gap of 10 meV. The electronic structure for the bilayer α-BNyne(2) is also presented in Figure 9(c). Similar to the single layer, the double-layered structure also has a wide band gap.

■ CONCLUSION

In conclusion, we investigated the cohesion, structural stabilities, electronic structures, and mechanical properties and functionalization by adatoms of α-graphyne(n) structures along with their h-BN analogues α-BNyne(n). By performing both phonon frequency and finite-temperature molecular dynamics analysis for n = 1−4 cases, we showed that both α-graphyne and α-BNyne are stable structures for even n but unstable for odd n. Interestingly, α-graphyne(3) undergoes a structural transformation to acquire stability, whereby the symmetry of hexagons forming honeycomb structure is broken. Thus, our study clarified the question whether a 2D periodic α-graphyne and α-BNyne structure can be stable or not. We also calculated the electronic structures for each of these materials and showed that α-graphyne(n) structures having Dirac cones are ambipolar and their Fermi velocities decrease with increasing n. It is also implied that all atoms being chemically equivalent is not a prerequisite for the existence of Dirac cones in the electronic structure. Upon hydrogenation, the Dirac cones are replaced by a large band gap. Since the formation of a single hydrogen vacancy renders a magnetic moment of 1 μ_B, magnetic nanomaterials can be designed by creation of domains of hydrogen vacancies. Our calculations of mechanical properties revealed that α-graphyne and α-BNyne are not as stiff as graphene and the single-layer h-BN, but they are strong enough to sustain the technological applications.

We finally showed that it is also possible to have double layers of α-graphyne and α-BNyne structures. Both of these bilayer structures have AB type of stacking. It was found that the electronic structure of bilayer α-graphyne has a gap opening of 10 meV at the K-point of the BZ, as opposed to single-layer α-graphyne(2). On the other hand, the electronic structure of bilayer α-BNyne(2) contains a wide band gap, similar to a single-layer BN structure.

Briefly, we demonstrated that α-graphyne and α-BNyne nanostructures can form stable and durable 2D extended structures with interesting chemical and physical properties,

which are scaled by n. We believe that these stable 2D carbon and BN allotropes will attract interest because of their unique properties in the near future. In particular, they can be utilized as structural frameworks for various spintronic[51] and chemical applications.

■ AUTHOR INFORMATION

Corresponding Author
*E-mail: ongunozcelik@bilkent.edu.tr; ciraci@fen.bilkent.edu.tr.

Notes
The authors declare no competing financial interest.

■ ACKNOWLEDGMENTS

■ REFERENCES

(1) Novoselov, K. S.; Geim, A. K.; Morozov, S. V.; Jiang, D.; Zhang, Y.; Dubonos, S. V.; Grigorieva, I. V.; Firsov, A. A. *Science* **2004**, *306*, 666−669.
(2) Geim, A. K.; Novoselov, K. S. *Nat. Mater.* **2007**, *6*, 183−191.
(3) Zhang, Y.; Tan, Y. W.; Stormer, H. L.; Kim, P. *Nature (London)* **2005**, *438*, 201−204.
(4) Baughman, R. H.; Eckhardt, H.; Kertesz, M. J. *J. Chem. Phys.* **1987**, *87*, 6687−6698.
(5) Tongay, S.; Dag, S.; Durgun, E.; Senger, R. T.; Ciraci, S. *J. Phys.: Condens. Matter* **2005**, *17*, 3823−3836.
(6) Malko, D.; Neiss, C.; Vines, F.; Gorling, A. *Phys. Rev. Lett.* **2012**, *108*, 086804.
(7) Hirsch, A. *Nat. Mater.* **2010**, *9*, 868−871.
(8) Diederich, F. *Nature (London)* **1994**, *369*, 199−207.
(9) Diederich, F.; Kivala, M. *Adv. Mater.* **2010**, *22*, 803−812.
(10) Haley, M. M. *Pure Appl. Chem.* **2008**, *80*, 519−532.
(11) Kehoe, J. M.; Kiley, J. H.; English, J. J.; Johnson, C. A.; Petersen, R. C.; Haley, M. M. *Org. Lett.* **2000**, *2*, 969−972.
(12) Bunz, U. H. F.; Rubin, Y.; Tobe, Y. *Chem. Soc. Rev.* **1999**, *28*, 107−119.
(13) Liu, H.; Xu, J.; Li, Y.; Li, Y. *Acc. Chem. Res.* **2010**, *43*, 1496−1508.
(14) Topsakal, M.; Akturk, E.; Ciraci, S. *Phys. Rev. B* **2009**, *79*, 115442.
(15) Narita, N.; Nagai, S.; Suzuki, S.; Nakao, K. *Phys. Rev. B* **1998**, *58*, 11009−11014.
(16) Coluci, V. R.; Braga, S. F.; Legoas, S. B.; Galvao, D. S.; Baughman, R. H. *Phys. Rev. B* **2003**, *68*, 035430.
(17) Zhou, J.; Lv, K.; Wang, Q.; Chen, X. S.; Sun, Q.; Jena, P. *J. Chem. Phys.* **2011**, *134*, 174701.
(18) Pan, L. D.; Zhang, L. Z.; Song, B. Q.; Du, S. X.; Gao, H. J. *Appl. Phys. Lett.* **2011**, *98*, 173102.
(19) Malko, D.; Neiss, C.; Vines, F.; Gorling, A. *Phys. Rev. B* **2012**, *86*, 045443.
(20) Sahin, H.; Ataca, C.; Ciraci, S. *Appl. Phys. Lett.* **2009**, *95*, 222510.
(21) Blochl, P. E. *Phys. Rev. B* **1994**, *50*, 17953−17979.
(22) Kresse, G.; Hafner, J. *Phys. Rev. B* **1993**, *47*, 558−561.
(23) Kresse, G.; Furthmuller, J. *Phys. Rev. B* **1996**, *54*, 11169−11186.
(24) Perdew, J. P.; Chevary, J. A.; Vosko, S. H.; Jackson, K. A.; Pederson, M. R.; Singh, D. J.; Fiolhais, C. *Phys. Rev. B* **1992**, *46*, 6671−6687.
(25) Grimme, S. *J. Comput. Chem.* **2006**, *27*, 1787−1799.
(26) Monkhorst, H. J.; Pack, J. D. *J. Comput. Chem.* **1976**, *13*, 5188.

(27) Giannozzi, P. e. a. *J. Phys.: Condens. Matter* **2009**, *21*, 395502.
(28) Tongay, S.; Senger, R. T.; Dag, S.; Ciraci, S. *Phys. Rev. Lett.* **2004**, *93*, 136404.
(29) Pauling, L. *The Nature of the Chemical Bonds*, 3rd ed.; Cornell University Press: New York, 1960.
(30) Eisler, S.; Aaron, D.; Elliott, E.; Luu, T.; McDonald, R.; Hegmann, F. A.; Tykwinski, R. R. *J. Am. Chem. Soc.* **2005**, *127*, 2666−26676.
(31) Meyer, J. C.; Girit, C. O.; Crommmie, M. F.; Zettl, A. *Nature (London)* **2008**, *454*, 319−322.
(32) Chalifoux, W. A.; Tykwinski, R. R. *Nature Chem.* **2010**, *2*, 967−971.
(33) Kittel, C. *Introduction to Solid State Physics*, 8th ed.; John Wiley & Sons: New York, 1996.
(34) It should be noted that the infinite carbon chain can undergo a Peierls distortion; the energy is slightly lowered, and alternating carbon atoms are slightly displaced from their equilibrium positions in cumulene. At the end, the unit cell consisting of two atoms bound by short (triple) and long (single) bonds is doubled. This structure is called polyne.
(35) Tongay, S.; Durgun, E.; Ciraci, S. *Appl. Phys. Lett.* **2004**, *85*, 6179.
(36) Cahangirov, S.; Topsakal, M.; Ciraci, S. *Phys. Rev. B* **2010**, *82*, 195444.
(37) Cahangirov, S.; Topsakal, M.; Akturk, E.; Sahin, H.; Ciraci, S. *Phys. Rev. Lett.* **2009**, *102*, 236804.
(38) Ataca, C.; Ciraci, S. *Phys. Rev. B* **2011**, *83*, 235417.
(39) Özçelik, V. O.; Ciraci, S. *Phys. Rev. B* **2012**, *86*, 155421.
(40) Özçelik, V. O.; Cahangirov, S.; Ciraci, S. *Phys. Rev. B* **2012**, *85*, 235456.
(41) Topsakal, M.; Cahangirov, S.; Ciraci, S. *Appl. Phys. Lett.* **2010**, *96*, 091912.
(42) Cranford, S. W.; Buehler, M. J. *Carbon* **2011**, *49*, 4111−4121.
(43) Kang, J.; Li, J.; Wu, F.; Li, S. S.; Xia, J. B. *J. Phys. Chem. C* **2011**, *115*, 20466−20470.
(44) Lee, C.; Wei, X.; Kysar, J. W.; Hone, J. *Science* **2008**, *321*, 385−388.
(45) Sahin, H.; Ciraci, S. *Phys. Rev. B* **2011**, *84*, 035452.
(46) Sofo, J. O.; Chaudhari, A. S.; Barber, G. D. *Phys. Rev. B* **2007**, *75*, 153401.
(47) Averill, F. W.; Morris, J. R.; Cooper, V. R. *Phys. Rev. B* **2009**, *80*, 195411.
(48) Zheng, Q.; Luo, G.; Liu, Q.; Quhe, R.; Zheng, J.; Tang, K.; Gao, Z.; Nagase, S.; Lu, J. *Nanoscale* **2012**, *4*, 3990−3996.
(49) Björkman, T.; Gulans, A.; Krasheninnikov, A. V.; Nieminen, R. M. *Phys. Rev. Lett.* **2012**, *108*, 235501.
(50) Partoens, B.; Peeters, F. M. *Phys. Rev. B* **2006**, *74*, 075404.
(51) Durgun, E.; Senger, R. T.; Mehrez, H.; Dag, S.; Ciraci, S. *Europhys. Lett.* **2006**, *73*, 642−648.

2182

dx.doi.org/10.1021/jp3111869 | *J. Phys. Chem. C* 2013, 117, 2175−2182